www.amlett.com, www.vbripress.com/aml, DOI: 10.5185/amlett.2015.5877 Published online by the VBRI Press in 2015

SnO_2 nanoparticles synthesis via liquid-phase co-precipitation technique

G. T. Lamdhade[1*], F. C. Raghuwanshi[1], R. M. Agrawal[1], V. M. Balkhande[1], T. Shripathi[2]

[1]*Department of Physics, Vidya Bharati Mahavidyalaya Camp, C.K. Naidu Road, Amravati, Maharashtra 444602, India*
[2]*ESCA Lab and Molecular Spectroscopy Lab, UGC-DAE Consortium for Scientific Research, University Campus, Khandwa Road, Indore, Madhya Pradesh 452001, India*

[*]Corresponding author. Tel: (+91) 9404518185; E-mail: gtlamdhade@rediffmail.com

Received: 28 February 2015, Revised: 25 March 2015 and Accepted: 29 March 2015

ABSTRACT

The samples have been prepared in the form of pellets of SnO_2 nanoparticles and synthesized via the liquid-phase co-precipitation technique. The ac electrical conductivity of samples is found to be frequency dependent. The dielectric constant increases with temperature and decreases with frequency of applied field. The semiconducting behavior of SnO_2 nanoparticles have been studied from I-V characteristics. The characterization of samples has been studied by XRD, FESEM, UV-spectra and TG-DTA plot. Copyright © 2015 VBRI Press.

Keywords: SnO_2 nanoparticles; liquid-phase synthesis; ac conductivity; dielectric constant; dielectric loss.

Introduction

Stannic oxide (SnO_2) is a wideband gap n-type semiconductor exhibiting rutile structure [**1**]. SnO_2 is applicable to the large number of field such as sensors, humidity sensors, optoelectronic devices, transparent electrodes, Li-ion batteries, etc **[2-6]**.

Single SnO_2 nanowire have been synthesized by thermal evaporation method and its I-V characteristics show semiconducting behavior , these nanowires would be a promising candidate for gas sensing applications due to its structural and electrical properties **[7]**. Nanocrystalline composites of Zinc oxide and Tin oxide synthesize by using chemical route and the sensing response characteristics for NO_2 gas has been studied and compared with corresponding results obtained for pure SnO_2 and ZnO thin film based sensor structure **[8]**. Thick film resistors of nano-phase SnO_2 powder have been prepared by using screen printing method and their surfaces were modified by dip coating in platinum chloride solution different time periods. The sensors were found to be extremely stable and repeatable **[9]**. Tin oxide quantum dots have been synthesized by solution-combustion method and there is formation of a rutile SnO_2 phase with a tetragonal lattice structure. The origin of the blue emission in the SnO_2 quantum dots is studied with reference to the energy band diagram **[10]**.

The properties of nanostructure material can be oriented as per requirements can be achieve by using the various experimental process for synthesis of nanoparticles such as chemical precipitation, sol–gel, hydrothermal, microwave technique, spray pyrolysis, CVD, etc **[11, 12]**.

Bueno *et al.* [**13**] investigated the AC electrical properties of tin oxide found that the two time constants with different activation energies, one at low frequencies and the other at high frequencies. AC transport properties of nanocrystalline tin oxide were studied by Sahay *et al.* [**14, 15**]**,** show that it is frequency dependent and obey the power law. The AC electrical conductivity of nanocrystalline tin oxide is found to be frequency dependent at a temperature of 200 °C and the result are interpreted in terms of the random potential barrier model **[16]**. As per the literature survey, there is less attention towards AC electrical, dielectric properties of nanocrystalline tin oxide as compared to DC conductivities mechanism **[17]**. This paper is devoted to effective method for the synthesis of nanocrystalline tin oxide using liquid phase co-precipitation method and AC electrical, dielectric measurements in the temperature range (313-473 K) were carried out in the frequency range (20 Hz - 1 MHz) , I-V characteristics, crystallographic structural (X-RD), morphological behavior (FESEM) and UV-vis absorbance spectrum are reported.

Experimental

Materials

All the chemicals used in this present work were of GR grade purchased from Sd-fine chemicals, India having purity 99.99% except conducting silver paint purchased from Sigma Aldrich Chemical, USA. Stannous chloride dehydrates ($SnCl_2.2H_2O$), ammonia solution and deionised water were used during reaction. The conducting silver paint is used to form electrodes during the experimental work.

Method of Preparation

In preparation of SnO_2, 2 g (0.1 M) of stannous chloride dihydrate ($SnCl_2.2H_2O$) is dissolved in 100 ml water. After complete dissolution, about 4 ml ammonia solution is added to above aqueous solution with magnetic stirring. Stirring is continued for 20 minutes. White gel precipitate is immediately formed. It is allowed to settle for 12 hours. Then it is filtered and washed with water 2-3 times by using deionised water. The obtain precipitate were mixed with 0.27 g carbon black powder (charcoal activated). The obtained mixer is kept in vacuum oven at 70ºC for 24 hours so that the mixer gets completely in to dried powder. Then this dry product was crushed into a find powder by grinder. Now obtained product of fine nanopowder of SnO_2 was calcinated at 700ºC up-to 6 hours in the auto controlled muffle furnace (Gayatri Scientific, Mumbai, India.) so that the impurities from product will be completely removed. The pellets of SnO_2 nanopowder were prepared by using electrically operated automatic press machine (Kbr Press) at load of 5 tons / cm^2 for half an hour. All the pellets were sintered at 150ºC for half an hour. The sintered pellets were polished and the electrodes were formed by painting conductive silver paint on the opposite faces. Again pellets were sintered for the drying the silver paint at 100ºC for half an hour.

Measurement of AC electrical conductivity and dielectric constant

The pellets of SnO_2 nanoparticles having diameter 12 mm and thickness 1.19 mm are placed in the silver electrodes sample holder (Pusha Scientific, Hyderabad, India) kept in electric oven to attained desired temperature. The samples is interlink to a precision LCR meter (20 Hz –1 MHz) (Model No. 4284 A, Agilent Technologies, Singapore), the corresponding effective capacitance (C_p) and effective resistance (R_p) measure at different environment of temperature recorded, finally the dielectric constants and ac electrical conductivity of the samples was calculated using expression **[18]**,

$$\sigma_{ac} = (f\, \varepsilon' \tan(\delta)) / (1.8 \times 10^{10}) \quad (1)$$

where, f is the frequency applied field in Hz, (ε') is the dielectric constant or relative permittivity and tan (δ) is the dielectric loss tangent or loss factor.

The values of the real part of the dielectric constant (ε') at different frequencies and temperatures were derived from the measured capacitance (C_p) and knowing the geometrical dimensions of the pellets using the expression,

$$\varepsilon' = (C_p L) / (\varepsilon_o A) \quad (2)$$

where, C_p is the measured capacitance, *L* is the thickness of the sample, A is the electrode area and (ε_o) is the permittivity of free space (8.854 X 10^{-12} F/m).

The dielectric loss tangent or dielectric loss factor i.e. tan (δ) can be expressed by relation,

$$\tan(\delta) = \omega . C_p . R_p \quad (3)$$

where, C_p is the measured capacitance, R_p is the measured resistance and f is the frequency applied field in Hz.

Measurement of current voltage characteristics

The current voltage (I-V) characteristics of SnO_2 nanoparticles were measured by using Source meter (Keithey Model No. 2400) in the temperature range (313 - 473 K). The samples are in the form of bulk pellets having diameter 12 mm and thickness 1.19 mm.

Characterization of SnO_2 nanoparticles

The crystalline nature of (SnO_2) nanoparticles was investigated using XRD. The XRD patterns were recorded on a Siemens D 5000 diffractometer with Cu-Kα radiation (λ=1.54060Å), over the range of 2θ = 5 - 80° at ambient temperature. Using Leica's SEM (Model S440) at 10kV, the morphology of (SnO_2) nanoparticles at room temperature was studied. Using UV-visible absorption spectrum of (SnO_2) nanoparticles are recorded on Shimadzu 1800 spectrophotometer at room temperature was studied.

Results and discussion

XRD pattern of the SnO_2 nanoparticles

The crystalline nature of the SnO_2 can be confirmed by the XRD pattern as shown in the **Fig. 1**. We observed the all peaks are perfectly matches with the JCPDS Data Card No. 77-0452, which indicating the present structure is found to be of SnO_2, which exist in the tetragonal rutile crystalline phase. The lattice parameters of the crystal were calculated as a = 0.4739 nm and c = 0.3221 nm which matches well with the standard values of SnO_2. The average crystalline size calculated by using Debye–Scherrer formula is found to be 21 nm for the three major peaks at (110), (101), (211) the crystal planes from the XRD pattern **[19]**. The average crystalline size was calculated by using Scherrer's formula given by equation **(4),**

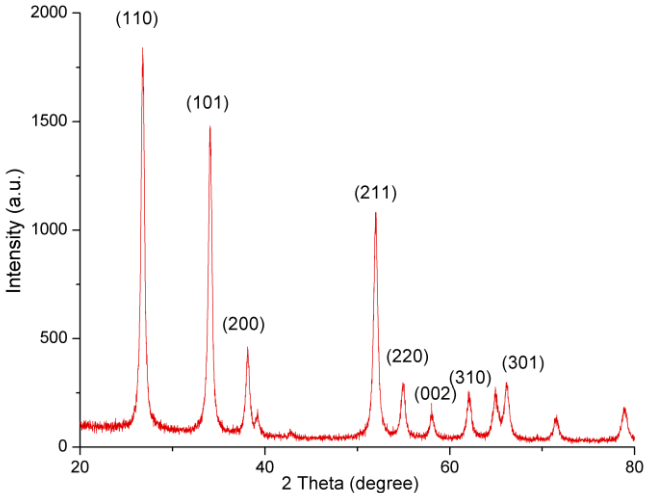

Fig. 1. XRD pattern of the SnO_2 nanoparticles.

$$D = \frac{K\lambda}{\beta\cos\theta} \quad (4)$$

where, D is the crystalline size, K is the shape factor and β is the full width at half maximum of diffraction angle in radians.

AC electrical conductivity and dielectric constant

The **Fig. 2** shows the variation between log of ac conductivity and applied frequency (20 Hz - 1 MHz) at different temperature (313 K, 353 K, 393 K, 433 K and 473 K) of the samples. The ac electrical conductivity of SnO_2 nanoparticles found to be frequency dependence which increases sharply from 20 Hz to 1 KHz frequency but beyond that it increase linearly with applied frequency. The frequency dependence of ac conductivity also obeys the power law relation [**20**]. The frequency dependence of ac conductivity of SnO_2 nanoparticles can be explained on the basis of Jonscher's classical equation [**21**] which shows the real part of ac conductivity has been frequency dependence. The another mechanism can also be explain on the basis of quantum-mechanical tunneling (QMT) through the barrier and classical hopping over the barrier [**22**]. It is also noted that due to increase in the temperature of samples, mobility of hopping ions increases which causing the increase in the conductivity with increase in the temperature.

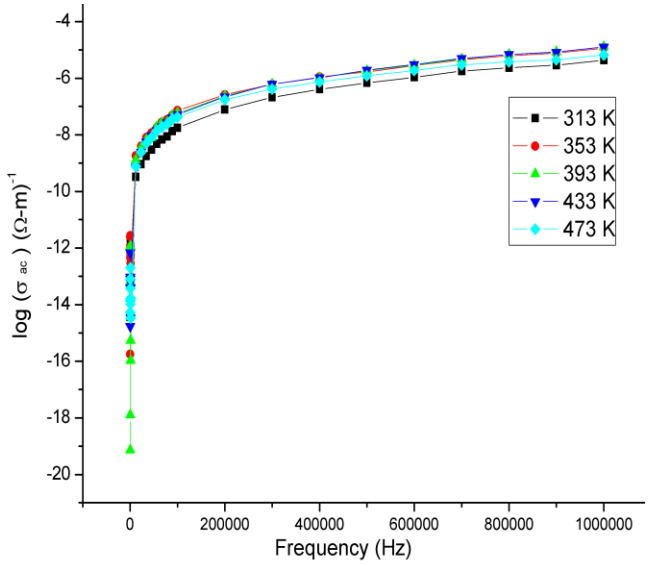

Fig. 2.Variation between log of ac conductivity and applied frequency.

The values of the real part of the dielectric constant (ε') at different frequencies and temperatures were derived from the **Eq. (2).** The variation of real part of the dielectric constant (ε') of SnO_2 nanoparticles with frequency of the applied field is plotted in the **Fig. 3** at constant temperature. These values can be obtained from the **Eq. (2).** It is clearly observed that the dielectric constant is found to decrease very rapidly from 20 Hz to 1 KHz frequency, but after 200 KHz frequency dielectric constant decreases very slowly up to 1 MHz frequency at all the constant temperature. In a dielectric study, the real part of dielectric constant (ε′) represents the polarizability of the material while the imaginary part (ε′′) represents the energy loss due to polarization and ionic conduction [**23**].

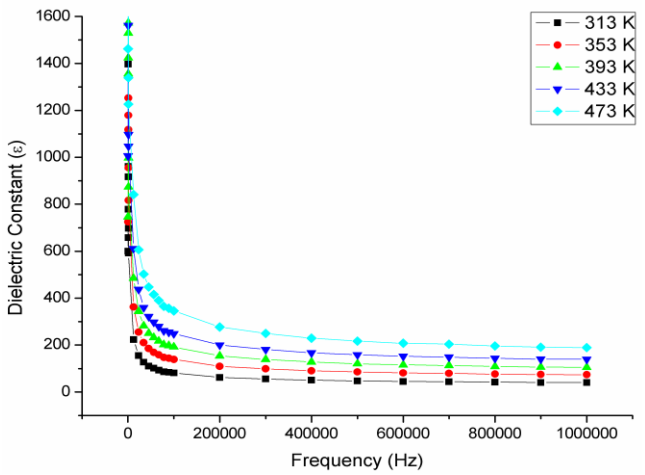

Fig. 3. Variation of dielectric constant (ε') with frequency of the applied field.

Dielectric loss factor (tan δ)

The **Fig. 4** shows the variation of dielectric loss factor (tan δ) of SnO_2 nanoparticles with applied field frequency (from 20 Hz to 1 MHz) at the different constant temperature. The values of the dielectric loss factor (tan δ) were derived from the eq. (3) which measures a part of polarization, which is out of phase with the applied field. Goldstone Mode (GM) relaxation and Soft Mode (SM) relaxation **[24]** are two types of rotational fluctuations of molecular dipoles. In the present study, the Goldstone Mode (GM) relaxation fluctuation are found be near the 200 Hz frequency while Soft Mode (SM) relaxation fluctuation are said to be absent.

It is also seen that dielectric constant and Dielectric loss factor (tan δ) increases with the increase in temperature for all the frequencies. When the temperature of samples increases, then its dipoles are more free accessible and easily react to the applied electric field, result of this the polarization will be increased, therefore the dielectric constant also increases with the increase in temperature **[25]**.

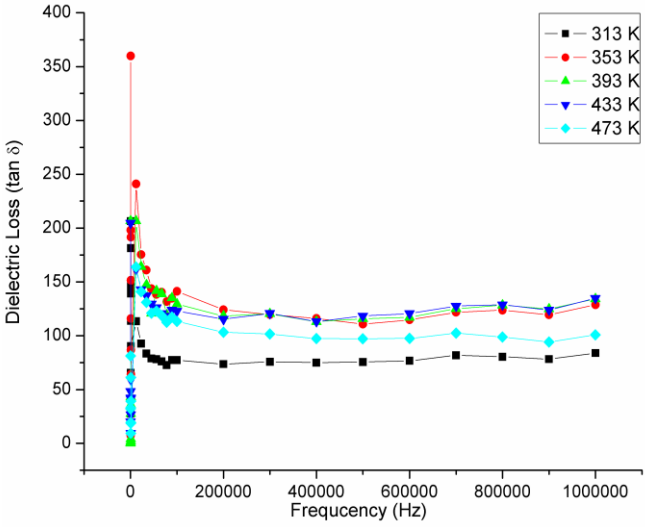

Fig. 4. Variation of dielectric loss factor (tan δ) with applied field frequency.

Current voltage characteristics

The **Fig. 5** shows I-V characteristics of SnO_2 nanoparticles at temperature range 313 - 473 K. The nature of plot shows the semiconducting behavior and obeys Ohms Law at temperature range 313 - 473 K. The semiconducting behavior of SnO_2 nanoparticles plays very important role in the gas sensing characteristics **[26]**. Therefore SnO_2 is said to be an promising candidate for the chemical gas sensors. The resistance of SnO_2 nanoparticles is found to be 2.29 MΩ at 473 K temperature.

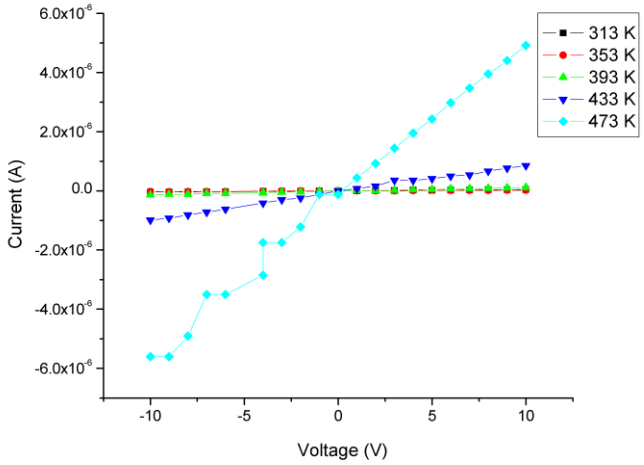

Fig. 5. I-V characteristics of the SnO_2 nanoparticles at temperature range (313-473 K).

Field emission scanning electron microscopy (FESEM)

The morphology and particle size of the prepared SnO_2 samples were determined by FESEM analysis as shown in **Fig. 6** which shows the FESEM picture of SnO_2 nanoparticles synthesized by using Liquid-phase method via co-precipitation. It is observed from micrographs, particles are found to be in the tetragonal shape within the particle size in the range about 15 - 31.2 nm. The average particle size observed in both FESEM and XRD measurement were found to be nearly equal.

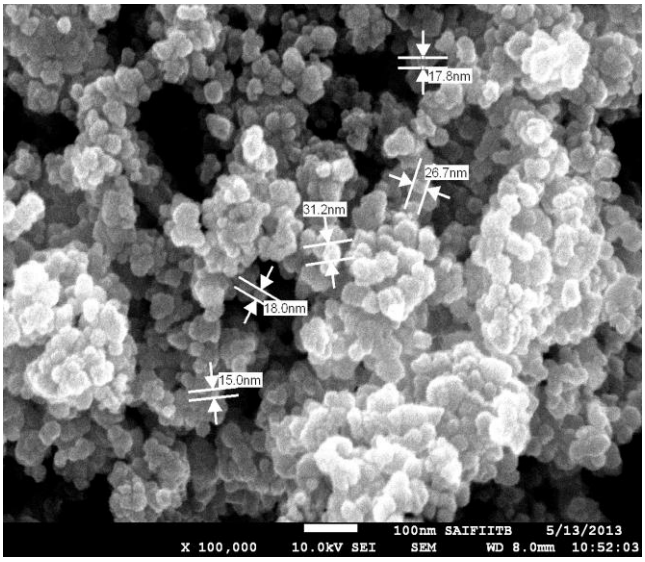

Fig. 6. FESEM picture of the SnO_2 nanoparticles.

UV-visible absorption spectrum

UV-visible absorption spectroscopy is widely used tool for checking the optical properties of nanosized particles. **Fig. 7** shows the UV-visible absorption spectrum of SnO_2 nanoparticles calcinated at temperature 700°C for 6 hours. From the spectrum four peaks are observed at 225 nm, 306 nm, 731 nm and 761 nm, out of this at 306 nm wavelength has been found maximum absorption, optical band gap for this wavelength found to be 4.05 eV, which is higher than the reported value of the bulk SnO_2, i.e. 3.6 eV **[27]**. This small difference in the optical band gap may be indicating that some impurity bands are developed near conduction bands **[28]**.

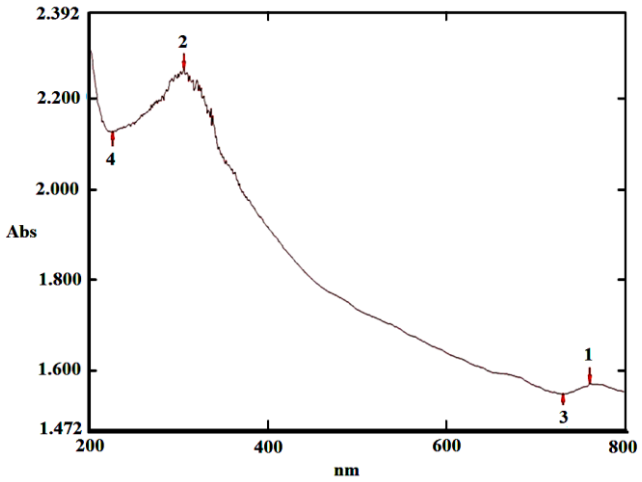

Fig. 7. UV-visible absorption spectrum of the SnO_2 nanoparticles.

TG-DTA plots

As shown in **Fig. 8**, show TG-DTA plots for pure SnO_2, which shows significant loss of weight is observed from room temperature to 500°C without plateau. The total rate of decomposition is found to be 0.52 mg/°C and total loss is 6 %. The endothermic peak on DTA curve is observed at 39°C which is associated with surface water loss. The small exothermic peak is observed at 490°C which may be attributed to phase change.

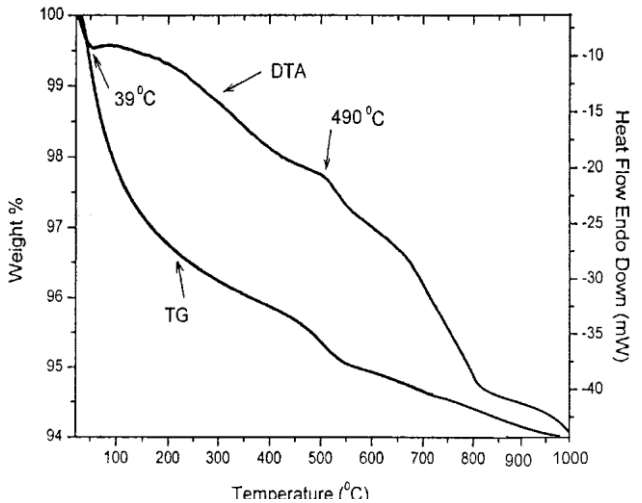

Fig. 8. TG-DTA plots for pure SnO_2.

From TG-DTA curves, upto 100^0C, loss of weight is due to loss of water contents in the sample. Weight loss is in the range ~0.5 to 4%. Onwards 100^0C upto 800^0C, the weight loss observed upto 12 %. During this temperature range the samples are found to be stable. After 800^0C, a sudden weight loss observed upto 6% which is due to transformation of $SnO \rightarrow Sn_3O_4$ during heating of the powder sample **[29].**

Conclusion

Preparation of SnO_2 nanostructures by using liquid-phase co-precipitation method is fast and easy. The ac electrical conductivity and dielectric constant has been frequency dependent. Tetragonal rutile crystalline phase, morphology of SnO_2 has been identified by XRD and FESEM respectively. The optical band gap is found to be 4.05eV**.** The significant loss of weight is observed from room temperature to 500 ^{0}C without plateau.

Acknowledgements

Authors are very much thankful to the Principal and Head Department of Physics both from Vidya Bharati Mahavidyalaya, Amravati for providing necessary laboratories facilities and also thankful to SAIF, Indian Institute of Technology, Bombay, Powai, Mumbai for providing the characterization of samples.

Reference

1. Rockenberger, J.; Felde, U.; M. Tischer, L.; Troger, M.; Haase, H.; Weller; *J. Chem. Phys.*, **2000**, *112*, 4296. **DOI:** 10.1063/1.480975
2. Seiyama, T.; Kato A.; Fujiishi, K.; Nagatani, M.; *Anal. Chem.*, **1962**, *34*, 1502. **DOI:** 10.1021/ac60191a001
3. Shukla, S.K.; Mishra, A.K.; Arotiba, O.A.; Mamba, B.B.; *Enzymes Microb. Technol.* **2014**, *66*, 48. **DOI:** 10.1016/j.enzmictec.2014.08.003
4. Zhang, J.; Gao, L.J.; *Solid State Chem*. **2004**, *177*, 1425. **DOI:** 10.1016/j.jssc.2003.11.024
5. Wang, Y.; Lee, J.Y.; *J. Phys. Chem*. B **2004,** *108*, 13589. **DOI**: 10.1021/jp048454w
6. Bhagwat. M.; Shah, P.; Ramaswamy, V.; *Mater. Lett.* **2003,** *57*, 1604. **DOI:** 10.1016/s0167-577x(02)01040-6
7. Johari A.; Bhatnagar, M.C.; Rana, V.; *Adv. Mat. Lett*. **2012**, *3(6)***,** 515. **DOI:** 10.5185/amlett.2012.icnano.251
8. Sonker, R.K.; Sharma, A.; Shahabuddin, Md.; Tomar, M.; Gupta, V.; *Adv. Mat. Lett*. **2013**, *4(3)*, 196. **DOI:** 10.5185/amlett.2012.7390
9. Garje, A.D.; Sadakale S.N.; *Adv. Mat. Lett*. **2013**, *4(1)*, 58. **DOI:** 10.5185/amlett.2013.icnano.228
10. Kumar, V.; Kumar, V.; Som, S.; Neethling, J.H.; Lee, M.; Ntwaeaborwa, O.M.; Swart, H.C.; *Nanotechnology*. **2014**, *25(13)*, 135701. **DOI:** 10.1088/0957-4484/25/13/135701
11. Ristic, M.; Ivanda, M.; Popovic, S.; Music, S.; *J. Non-Cryst. Solids*, **2002**, *303*, 270. **DOI:** 10.1016/s0022-3093(02)00944-4
12. Liu, Y.; Koep, E.; Liu, M.; *Chem. Mater*. **2005**, *17*, 3997. **DOI:** 10.1021/cm050451o
13. Bueno, P. R .; Pianaro, S.A.; Pereira, E.C.; Bulhoes, L.O.S.; Longo, E.; Varela, J.A.; *J. Appl.Phys.*, **1998**, *84*, 3700. **DOI:** 10.1063/1.368587
14. Sahay, P.P.; Mishra, R.K.; Pandey, S.N.; Jha, S.; Shamsuddin, M.; *Ceramics Int.* **2012**, *38(2)* , 1281. **DOI:** 10.1016/j.ceramint.2011.08.062
15. Sahay, P. P.; Mishra, R.K.; Pandey, S.N.; Jha, S.; Shamsuddin, M.; Current *Appl. Phys.***2013**, *13(3)*, 479. **DOI:** 10.1016/j.cap.2012.09.010
16. Chizhov, A.; Rumyantseva, M.; Gaskov, A.*; Inorg. Mat.* **2013**, *49(10)*, 1000. **DOI:** 10.1134/s0020168513100014
17. Ni, J.; Zhao, X.; Zheng, X.; Zhao, J.; Liu, B. ; *Acta Mater.* **2009**, *57*, 278. **DOI:** 10.1016/j.actamat.2008.09.013
18. Vijayalakshmi, R.; Ashokan, P.V.; Shridhar, M.H. ; *Mat. Sci. Eng. A* **2000**, *281*, 213. **DOI:** 10.1016/s0921-5093(99)00723-6
19. Cullity, B.D.; *Elements of X-ray diffraction* (Addison-Wesley), **1970,** 102. **DOI:** 10.1119/1.1934486
20. Butcher, P.N.; Morys, P.L.; *J. Phys. C, Solid State Phys*., **1973**, *6*, 2147. **DOI:** 10.1088/0022-3719/6/13/014
21. Ce-Wen, N.; Holten, S.; Birringer, R.; Haibin, G. ; Kliem, H.; Gleiter, H.; *Phys. stat. sol.* **1997**, *(a) 164 No.1* , R1-R2. **DOI:** 10.1002/1521-396x(199711)164:13.0.co;2-#
22. Elliot, S.R.; *Adv. Phys.* **1987**, *36*, 135.
23. Saltas, V.; Vallianatos, F.; Soupios, P.; Makris, J.P.; Triantis, D.; *J. Hazard. Mater.* , **2007**, *142*, 520. **DOI:** 10.1016/j.jhazmat.2006.08.051
24. Singh, D.P.; Gupta, S.K.; Pandey, A.C.; Manohar, R.; *Adv. Mat. Lett.* , **2013**, *4(7)*, 556. **DOI:** 10.5185/amlett.2012.11463.
25. Frohlick, H.; Theory of Dielectrics; Oxford University press, **1956**.
26. Johari A.; Rana V.; Bhatnagar M. C.; *Nanomater; nanotechnol.*, **2011,** *1(2)* ,49. **DOI**: 10.1109/inec.2011.5991739
27. Fang, L.M.; Zu, X.T.; Li, Z.J.; Zhu, S.; Liu, C.M.; Wang, L.M.; Gao, F.; *J. Mater. Sci: Mater. Electron*, **2008,** *19* , 868. **DOI:** 10.1007/s10854-007-9543-7
28. Terrier, C.; Chatelon, J.P.; Roger, J.A.; *Thin Solid Films*, **1997**, *295*, 95. **DOI:** 10.1016/s0040-6090(96)09324-8
29. Madhusudhana Reddy, M.H.; Jawalekar, S.R; Chandorkar A.N.; *Thin solid films*, **1989**, *169*, 117. **DOI:** 10.1016/s0040-6090(89)80010-0